BioMedical Engineering OnLine

CrossMark

RESEARCH

Development and performance analysis of Si-CaP/fine particulate bone powder combined grafts for bone regeneration

Chengli Sun[1†], Ye Tian[2†], Wenxiao Xu[2], Changlong Zhou[2], Huanxin Xie[2] and Xintao Wang[2*]

*Correspondence: xintaog6@163.com
†Chengli Sun and Ye Tian contributed equally to this work.
[2] Department of Orthopaedic Surgery, The Second Affiliated Hospital of Harbin Medical University, 246 Xuefu Street, Nangang District, Harbin 150086, China
Full list of author information is available at the end of the article

Abstract

Background: Although autogenous bone grafts as well as several bone graft substitute material have been used for some time, there is high demand for more efficient and less costly bone-substitute materials. Silicon-substituted calcium phosphates (Si-CaP) and fine particulate bone powder (FPBP) preparations have been previously shown to individually possess many of the required features of a bone graft substitute scaffold. However, when applied individually, these two materials fall short of an ideal substitute material. We investigated a new concept of combining Si-CaP with FPBP for improved performance in bone-repair.

Methods: We assessed Si-CaP/FPBP combined grafts in vitro, by measuring changes in pH, weight loss, water absorption and compressive strength over time.

Results: Si-CaP/FPBP combined grafts was found to produce conditions of alkaline pH levels compared to FPBP, and scaffold surface morphology conducive to bone cell adhesion, proliferation, differentiation, tissue growth and transport of nutrients, while maintaining elasticity and mechanical strength and degradation at a rate closer to osteogenesis.

Conclusion: Si-CaP/FPBP combined grafts was found to be superior to any of the two components individually.

Keywords: Si-CaP, Fine particulate bone powder, Bone regeneration

Background

The repair and regeneration of bone is a complex interplay between the ground substance, cells and milieu, but is still not fully comprehended [1]. Although autologous bone grafts have been used successfully for many bone disorders for some time now, it is not always practical and can be challenging in harvesting sufficient graft material and causes trauma to the donor site.

There are alternative materials to autologous bone grafts currently used in various bone repairs that have yielded some success. However, there are many technical problems and the osteogenic effect of such alternatives is still not satisfactory [2, 3]. Natural biological materials such as collagen, chitosan and others have problems such as poor

Sun *et al. BioMed Eng OnLine* (2015) 14:47

Page 2 of 14

mechanical strength, immunogenicity, non-osteoconductivity or non-osteoinducive, inappropriate degradation time or poor reproducibility [4, 5].

Organic polymers such as poly(lactic acid), poly(glycolic acid), poly(ε-caprolactone) and poly(lactic-co-glycolic acid) copolymers have insufficient mechanical strength and are poorly hydrophilic. Degradation of some organic polymers causes acidic conditions that result in inflammation. These materials also have weak adsorption of cells and more importantly: lack cell surface recognition signals and interaction with the biological tissue. In addition, they are still expensive and have unsatisfactory plasticity [1, 6].

With inorganic materials such as β-tricalcium phosphate, hydroxyapatite, and bioactive glass, the scaffold resorption rate exceeds the bone formation rate and cannot maintain repair function. Others absorb too slowly or not at all, can produce foreign body reactions after implantation, are not conducive to new bone remodeling and their production method cannot guarantee consistent pore connectivity [1, 7]. Therefore, alternatives to autogenous bone graft material to accelerate the repair of bone defects has been an important issue faced by orthopedic surgeons.

Calcium phosphate has been commonly used as a substitute scaffold in bone tissue engineering, but easily becomes brittle, has poor degradation performance and absorbs poorly, affecting the formation of new bone and later development [8, 9]. However, silicon-substituted calcium phosphate (Si-CaP) has been found to have good biocompatibility, biodegradability and osteoconduction [10, 11]. The addition of silicone to calcium phosphates causes changes in the structural properties of the scaffolding material and significantly improves bioactivity. These materials become fully absorbed by bone cells and are replaced by natural bone during bone remodeling [12, 13]. Several studies [14–20] have shown that, compared with a pure calcium phosphate, Si-CaPs have the following advantages: (1) good degradation performance, (2) higher biological activity, (3) supports the migration of bone cells and their differentiation and (4) can reduce cell damage caused by environmental changes. Si-CaP is a new scaffold with good prospects. However, although Si-CaP is osteoconducive, it is not osteoinducive [21], which is a major shortcoming of autogenous bone graft substitute materials. Creating a scaffold that is combined with a substance that is involved in osteoinduction may increase the osteogenic potential of the graft substitute material. Studies have shown that fine particles of bone accelerate healing compared to traditional bone grafts [22]. However, since such particles of lose bone structure easily drain, are difficult to mold and have other shortcomings, the application is limited. Therefore, we focused on ways to overcome the respective shortcomings of Si-Cap and fine bone particles in bone repair. To do this, we investigated the potential of viable osteoblasts in fine particulate bone powder (FPBP) to provide osteoinductive and osteogenic properties to the osteoconductive Si-CaP in the combination scaffold: Si-CaP/FPBP, as a tentative method for bone-defect repair.

Methods

Synthesis and identification of Si-CaP

Three-dimensional porous Si-CaP tubes were prepared using aqueous precipitation method as described previously [23]. The tubes had an inside diameter, outside diameter and length of 0.6, 1 and 1.5 cm, respectively and weighed 1.5 g. The crystal phase composition of Si-CaP was studied with X-ray diffraction, using a D/MAX-Rb X-ray diffractometer

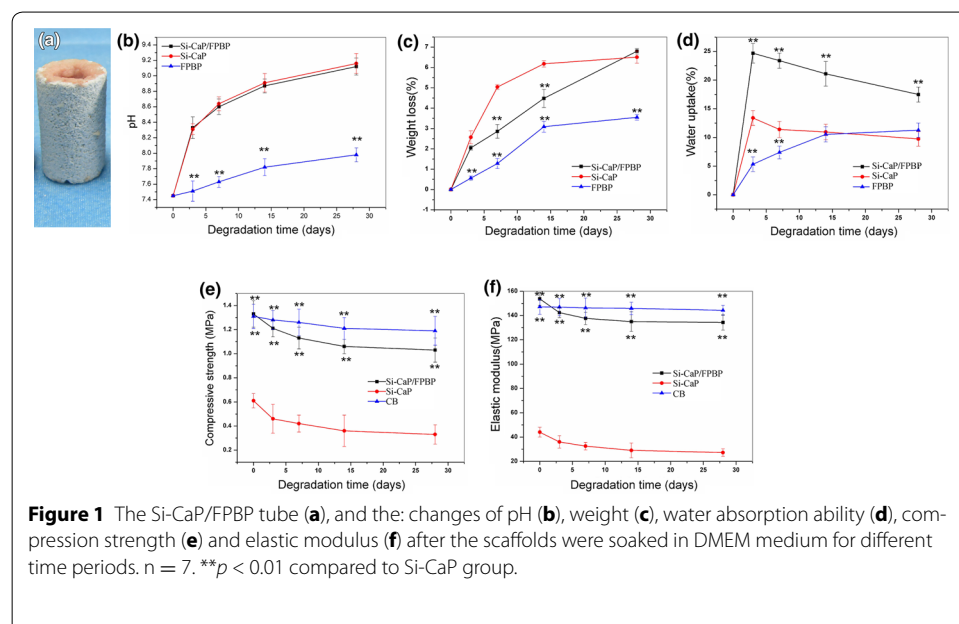Sun *et al. BioMed Eng OnLine* (2015) 14:47

Page 3 of 14

(Rigaku, Japan) with Ni-filtered Cuka radiation operated at 30 kV and 10 mA at a scanning speed of 1/min. Si-CaP functional groups were detected by Nicolet710 Far-infrared Fourier transform spectroscopy (Thermal, United States) with a frequency range from 4,000 to 400 cm^{-1} and a resolution of 2 cm^{-1}. Si-CaP microstructure and elemental composition was analyzed using a dual beam focused ion beam scanning electron microscopy (FIB-SEM) system (HELIOS NanoLab 600i, FEI, Netherlands) equipped with an energy dispersive X-ray spectroscopy (EDS) unit operated at 20 kV. Liquid displacement methodology was used to measure the porosity of Si-CaP as described previously [24].

Preparation of fine particulate bone powder

Animal study was approved by the Institutional Animal Care and Use Committee of Harbin Medical University (Protocol: 2012-002). FPBP was prepared from New Zealand white rabbits (6 months old, 2.5 kg). Briefly, iliac crest bone (1 g) was first ground using an electric ball mill drill (BJ2103, Bojin, China). Particles of 300–500 μm were isolated using a sub-sieve sizer and centrifuged at 120 rpm for 5 min (Eppendorf, Germany). Light microscopy (DVM2500, Lecia, Germany) and scanning electron microscopy (SEM) (HELIOS NanoLab 600i, FEI, Netherlands) were used to characterize the general and surface morphology of FPBP particles.

Construction of Si-CaP/FPBP scaffold

To prepare Si-CaP/FPBP scaffolds, Si-CaP and FPBP were mixed at a 1:1 weight ratio and packed into 1.6 cm^3 tubes (diameter: 0.92 cm, height: 2 cm). An example of the scaffold is shown in Figure 1a. Si-CaP, FPBP and Si-CaP/FPBP scaffolds were then subjected to in vitro degradation tests at 37°C. Experiments were divided into three groups: Si-CaP group, FPBP and Si-CaP/FPBP. Si-CaP tubes were filled with FPBP at a weight ratio of 1:1 (0.75 g of each component). Bone scaffolds were cultured in six well culture plates containing

Figure 1 The Si-CaP/FPBP tube (**a**), and the: changes of pH (**b**), weight (**c**), water absorption ability (**d**), compression strength (**e**) and elastic modulus (**f**) after the scaffolds were soaked in DMEM medium for different time periods. n = 7. **p < 0.01 compared to Si-CaP group.

Sun *et al. BioMed Eng OnLine* (2015) 14:47

Page 4 of 14

15 ml DMEM culture medium (pH 7.4) (Invitrogen, USA). Bone scaffolds were incubated at 37°C for 3, 7, 14 and 28 days.

pH measurement

The pH change of the culture medium was detected with pH meter at each at 0, 3, 7, 14 and 28 days of incubation. Each average pH value was obtained from seven measurements taken under the same testing conditions. Experiments were performed in seven replicates.

Weight loss

To measure the weight changes, scaffolds were removed from the culture plates at 0, 3, 7, 14 and 28 days of incubation, rinsed with water and dried for 24 h with a blow dryer. The weight loss values were measured using an electronic balance with an accuracy of 0.001 g. The weight loss ratio was calculated from the equation:

weight loss ratio (%) = $(M_0 - M_1)/M_0 \times 100,$

where M_0 is the weight of scaffolds before degradation and M_1 is the weight of dried scaffolds after degredation. Each average weight loss value was obtained from seven measurements taken under the same testing conditions. Experiments were performed in seven replicates.

Water absorption

Water absorption was measured at 0, 3, 7, 14 and 28 days of incubation. To measure the water absorption, scaffolds were removed from the culture plates and blotted dry on filter paper to remove excess water. The water absorption was measured using an electronic balance with an accuracy of 0.001 g. The water absorption ratio was calculated from the equation:

water absorption ratio (%) = $(M_2 - M_0)/M_0 \times 100,$

where M_2 is the weight of scaffolds with excess water removed. Each average water absorption value was obtained from seven measurements taken under the same testing conditions. Experiments were performed in seven replicates.

Compressive strength measurement

The compressive strengths of the scaffolds were determined using Electronic Universal Testing Machine (Instron 5500R, United States) with a crosshead speed of 1.0 mm/min. To conduct the test, the scaffolds were removed from the culture plates, rinsed with deionized water and dried thoroughly using a blow dryer. The load was recorded as compressive strength (MPa) at the point where the scaffold fractured. The elastic modulus (MPa) was determined by the slope of the initial linear portion of the stress–strain curve. Each average value was obtained from seven measurements taken under the same testing conditions. Experiments were performed in seven replicates.

Sun *et al. BioMed Eng OnLine* (2015) 14:47

Page 5 of 14

Surface morphology

The surface morphology of scaffolds were observed using FIB-SEM. Briefly, the scaffolds were removed from the culture plates, fixed with 2.5% glutaraldehyde solution (pH 7.4) (Sigma Chemical Co., USA) for 24 h at 4°C and then for 30 min in 1% osmium tetroxide (Sigma Chemical Co.). The scaffolds were dehydrated in a graded series of ethanol, critically point dried with CO_2 and sputtered with gold.

H&E staining

For H&E staining, nuclei was stained with alum haemtoxylin for 10 min and differentiate with 0.3% acid alcohol for 2 s. Then, samples were rinsed in Scott's tap water substitute and stained with eosin for 2 min. Finally, slides were dehydrated and mounted with permount medium.

Statistical analysis

All values were expressed as mean $\pm$ standard deviation. Differences among groups were analyzed by ANOVA followed by Bonferroni post hoc analyses as appropriate, using SPSS 17.0 statistical software. A p value of <0.05 was considered significant.

Results

Synthesis and identification of Si-CaP

X-ray diffraction analysis showed that synthesized Si-CaP was homogenous and single phase material with all peaks matching with standard Si-CaP diffraction peaks provided by the International Centre for Diffraction Data (Figure 2a). Far-infrared Fourier transform spectroscopy analysis of two batches of Si-CaP exhibited same absorbance spectrum with major bands at 1,125 and 692 cm^{-1}, demonstrating the repeatability of this synthesis method (Figure 2b). The images obtained from FIB-SEM showed rod or spherical shapes of Si-CaP particles with small Si-CaP crystals clustered on the surface (Figure 3a–c). Nanoscale pores with irregular sizes and shapes, formed by Si-CaP crystal clusters, were present on particle surfaces. Macropores of 150–300 μm were evenly distributed and connected by micropores of 1–10 μm throughout the scaffolds. EDS point analysis detected 8% silicon in the Si-CaP (Figure 3d; Table 1). Additionally, as determined by liquid displacement methodology, the average porosity of Si-CaP was 74.144 $\pm$ 3.833%.
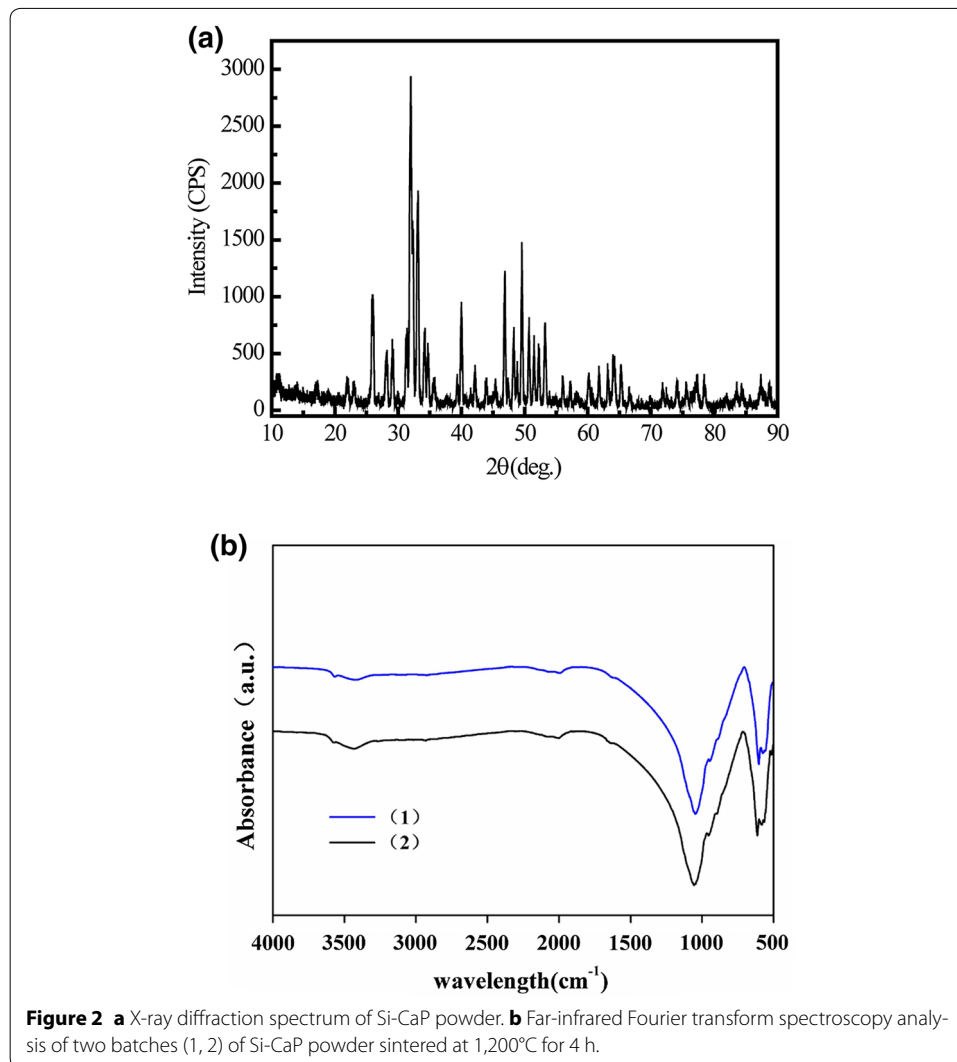
Preparation and characterization of FPBP

Bright field images showed that FPBP particles had irregular shape with bone debris scattered on the surface (Figure 4a). SEM was used to characterize the surface morphology of FPBP (Figure 4b, c). The FPBP was observed as a mixture of 10 μm porous cortical and cancellous bone. The majority was coarse cancellous bone.

Preparation and characterization of Si-CaP/FPBP scaffold

An example of the obtained Si-CaP/FPBP tubes is shown in Figure 1a.

pH change

The pH of DMEM solution during the in vitro degradation of three types of scaffolds was first determined. As degradation time increased, the pH of the DMEM solution in all three

Sun *et al. BioMed Eng OnLine* (2015) 14:47

Page 6 of 14

Figure 2 a X-ray diffraction spectrum of Si-CaP powder. **b** Far-infrared Fourier transform spectroscopy analysis of two batches (1, 2) of Si-CaP powder sintered at 1,200°C for 4 h.
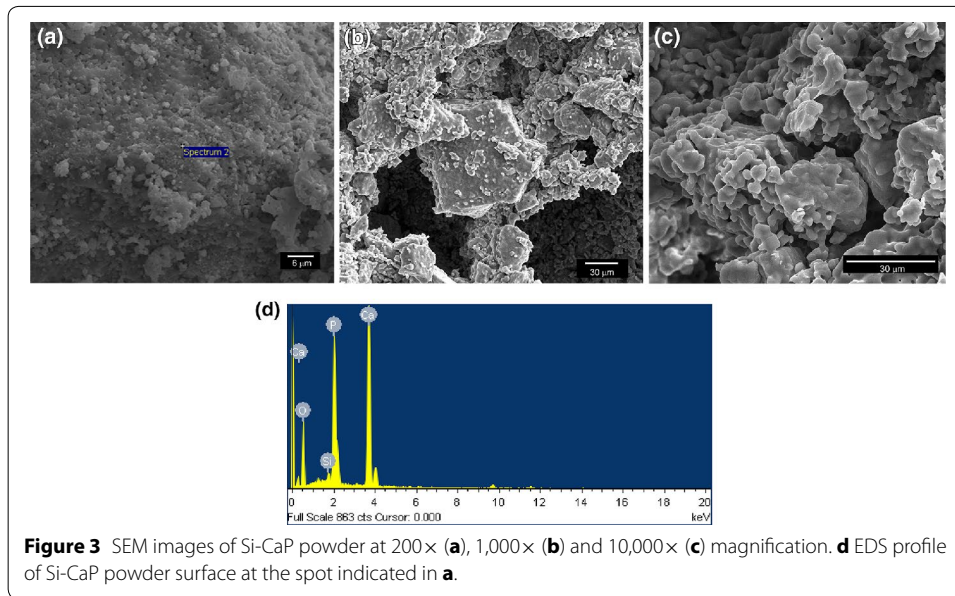
groups increased. The pH values of Si-CaP degradation solution were slightly higher than that of Si-CaP/FPBP degradation solution, but with no significant difference (P > 0.05). However, the pH values of both Si-CaP and Si-CaP/FPBP degradation solutions were significantly higher than the pH value of the FPBP solution (Figure 1b, P < 0.05).
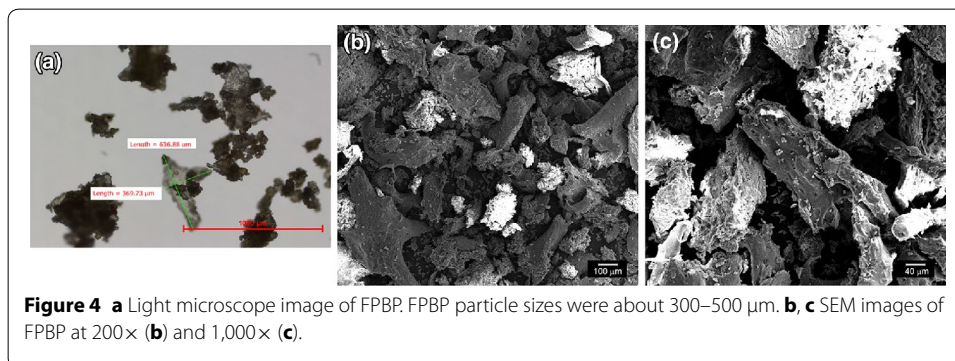
Weight loss

As shown in Figure 1c, Si-CaP and Si-CaP/FPBP scaffolds experienced dramatic weight loss during the 28 days of incubation. Si-CaP scaffolds degraded significantly faster than Si-CaP/FPBP composite scaffolds between days 3 and 14. In contrast, the FPBP group experienced significantly slower weight loss than both Si-CaP and Si-CaP/FPBP groups (P < 0.05).

Changes in water absorption

The water absorption of Si-CaP and Si-CaP/FPBP scaffolds can be divided into two phases during the in vitro degradation process: 0–3 days, water absorption increased significantly,

Sun *et al. BioMed Eng OnLine* (2015) 14:47

Page 7 of 14

Figure 3 SEM images of Si-CaP powder at 200× (**a**), 1,000× (**b**) and 10,000× (**c**) magnification. **d** EDS profile of Si-CaP powder surface at the spot indicated in **a**.

Table 1 Elemental analysis of Si-CaP by EDS

Element	Weight (%)
O K	50.09
Si K	0.8
P K	16.48
Ca K	32.63
Total	100.00

Figure 4 a Light microscope image of FPBP. FPBP particle sizes were about 300–500 μm. **b**, **c** SEM images of FPBP at 200× (**b**) and 1,000× (**c**).

and 3–28 days, water absorption appeared to decrease slowly. In contrast, water absorption by FPBP increased slowly, and after 14 days apparent water absorption did not change significantly. Overall, scaffolds in Si-CaP/FPBP group had the highest water uptake amongst the three groups (Figure 1d). However, water absorption was assessed by differences in weight and after 3 days, change in weight is likely due to scaffold-dissolution, rather than loss of absorbed water.

Sun *et al. BioMed Eng OnLine* (2015) 14:47

Page 8 of 14
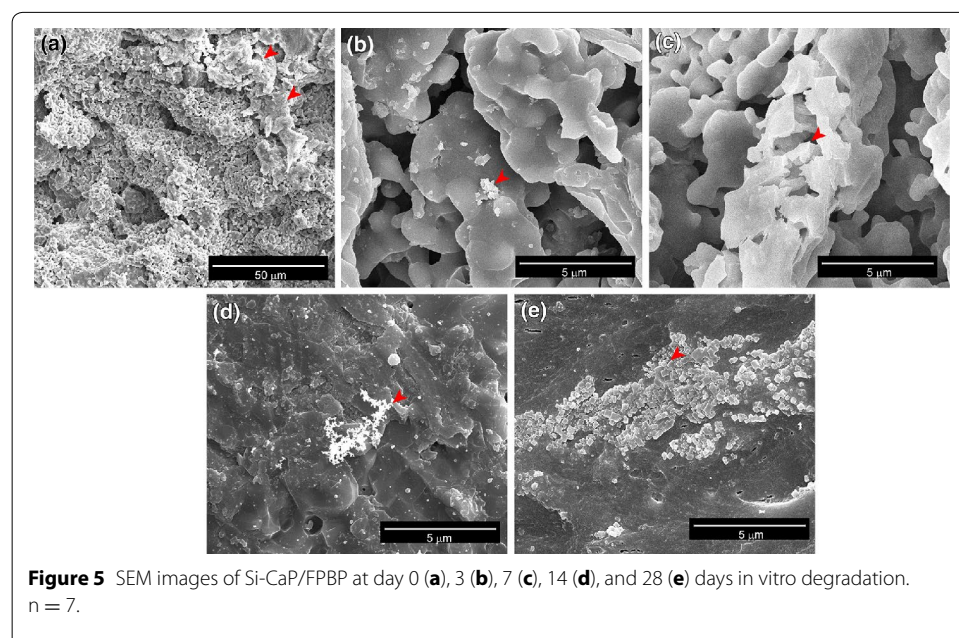
Compressive strength

The change in compressive strength of Si-CaP, Si-CaP/FPBP and cortical bone (CB) was measured and compared (Figure 1e). The strength of scaffolds in each group continuously decreased during the 28 day period. Before in vitro degradation, the average compression strength of Si-CaP/FPBP, Si-CaP and CB was 1.288 ± 0.107, 0.614 ± 0.130 and 1.200 ± 0.130 MPa, respectively. Before degradation, the compression strength of Si-CaP/FPBP scaffolds was significantly higher than that of Si-CaP scaffolds, but lower than that of CB blocks ($P < 0.05$).

Elasticity modulus

Before in vitro degradation, the elasticity modulus of Si-CaP/FPBP, Si-CaP and CB blocks were 149.705 ± 7.414, 43.033 ± 3.933 and 143.976 ± 4.630 MPa, respectively. The elasticity modulus of scaffolds in Si-CaP, Si-CaP/FPBP groups continuously decreased over the 28 days. As shown in Figure 1f, the elasticity modulus of Si-CaP was significantly lower than the Si-CaP/FPBP. The elasticity modulus of Si-CaP/FPBP scaffolds was slightly lower than CB blocks, but not significantly different ($P > 0.05$).

SEM observation of scaffolds

Cross-section surface morphology of Si-CaP/FPBP scaffold was observed with SEM before in vitro degradation. We found that FPBP attached tightly to the surface of Si-CaP particles (Figure 5a). Si-CaP particles showed uniform short rod shape with size of approximately 2–10 μm. Si-CaP particles and FPBP were relatively uniform and positioned closely together. The Si-CaP/FPBP scaffold formed three-dimensional porous structures. The sizes of pores were approximately 150–300 μm with micropores of 1–10 μm distributed on the relatively smooth pore wall.

Figure 5 SEM images of Si-CaP/FPBP at day 0 (**a**), 3 (**b**), 7 (**c**), 14 (**d**), and 28 (**e**) days in vitro degradation. n = 7.

Sun *et al. BioMed Eng OnLine (2015) 14:47*

Page 9 of 14

After 3 days degradation in DMEM medium, we found Si-CaP/FPBP scaffolds partially degraded and single small spherical particles deposited on the scaffold surface (Figure 5b). Each spherical particle was composed of several apatite crystals, observed by high-powered microscopy (data not shown). The Si-CaP and FPBP scaffolds showed no change (data not shown). At 7 days of in vitro incubation, we found the cell wall of Si-CaP/FPBP scaffold was degraded. Lamellar bone-like apatite had formed on the scaffold surface and a large number of small bone-like apatite particles were deposited on the pore wall (Figure 5c). At the same time point, Si-CaP and FPBP scaffolds surface was only slightly degraded. At 14 days of in vitro incubation, a large number of loose, spherical or short rod-like bone-like apatite particles had deposited on the surface of Si-CaP/FPBP scaffolds (Figure 5d). Finally, at 28 days, a large number of regular lamellar bone-like apatite particles with size approximately 0.2–1 μm were observed on the Si-CaP/FPBP surface (Figure 5e).

H&E observation

H&E observation found that Si-CaP and FPBP engaged tightly with each other at the interface on day 0. As time increased, Si-CaP at the junction between Si-CaP and FPBP became sparse and loose. Lacunae gradually became empty. After 14 days of in vitro incubation, osteoblasts had lyzed and disappeared (Figure 6a–e).

Discussion

Calcium phosphates are the most frequently used materials in bone substitutions today, due to their similarity to natural inorganic compounds in bone [25–27]. Patel et al. [28] showed that incorporation of silicate ions into hydroxyapatite significantly improves bioactivity. Here, we show that the combination of fine bone particles with silicone-calcium phosphate, further improves the performance of the scaffold.
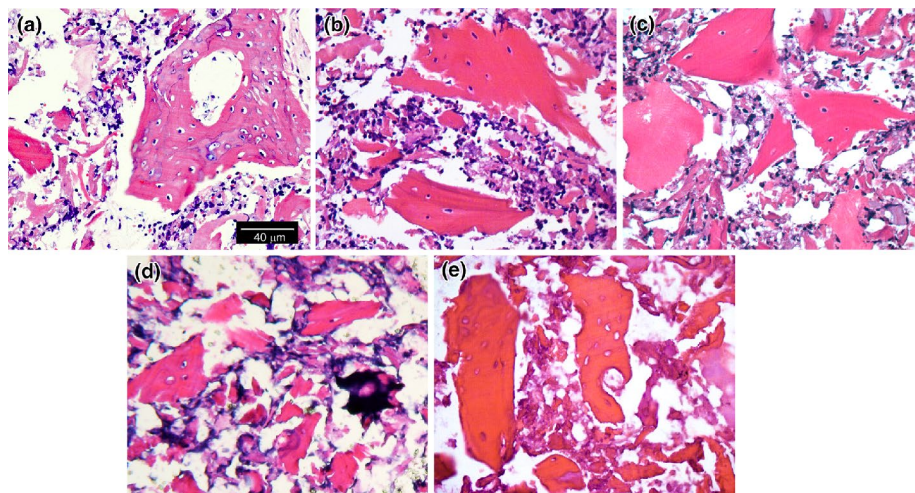

Figure 6 H&E images of Si-CaP/FPBP at day 0 (**a**), 3 (**b**), 7 (**c**), 14 (**d**), and 28 (**e**) days in vitro degradation. n = 7.

Sun *et al. BioMed Eng OnLine* (2015) 14:47

Page 10 of 14

Degradation and mechanical properties of Si-CaP/FPBP in vitro

Tuck et al. [25] performed a degradation experiment with Si-CaP in deionized water at a 1:30 mass to volume ratio. After 30 days, the pH of the water had increased from 7.4 to approximately 9 and stabilized there. Analysis by multiple methods showed that Si-CaP had good degradation performance and formed bone-like apatite in vitro. Similarly, the pH of the DMEM for the Si-CaP/FPBP group and the Si-CaP group in our experiment also increased significantly over time and reached approximately 9 after 28 days. FPBP alone only had a modest increase in pH. This change is mainly due to the interaction of oxygen in the phosphate group of the Si-CaP surface with water, producing hydroxide. The reaction is as follows: $PO_4^{3-} + H_2O = HPO_4^{2-} + OH^-$ [25]. Further to this, the dissolution of Si-CaP releases Ca^{2+} into the DMEM culture medium as the charge-compensating Si-CaP absorbs two H^+ ions, resulting in the pH of the DMEM culture increasing further [25]. The pH of Si-CaP/FPBP group was lower than the pH of Si-CaP group throughout the entire degradation process. This may be due to the interaction of Si-CaP with FPBP making the overall degradation rate relatively low and closer to osteogenesis. The surface of Si-CaP/FPBP scaffold degraded completely after 7 days and increasingly formed apatite deposition over the 28 days. The surface of FPBP and Si-CaP scaffolds had degraded slightly at 7 days of incubation with the deposition of some bone-like apatite particles, but there was no significant change after 28 days. This may be due the hydroxyapatite slowly dissolving and escaping from the FPBP. The ability of a scaffold to bond to the living material that surrounds it, as well as maintaining non-acid conditions, is essential to the healing process. The cross-linking of collagen chains during bone formation requires alkaline conditions [29]. Formation of bone-like apatite on the surface of a bone-substitute scaffold is crucial to bone-bonding and facilitates osteoblast adhesion and proliferation. In vitro evaluation of a material's apatite-forming ability also correlates well with its bone-bonding ability in vivo. Therefore, making in vitro observations of apatite formation is a useful way of preliminary screening of new scaffolding materials before in vivo assessment [28, 30, 31].

The weight loss of the Si-CaP, FPBP and Si-CaP/FPBP groups increased continually as incubation time increased, indicating that the three groups of materials degraded continually in DMEM. At 0–3 days of incubation, the degradation of the amorphous region of the amorphous phase in the Si-CaP group and Si-CaP/FPBP group resulted in the release of large amounts of degradation products, such as PO_4^{3-} and Ca^{2+}, and caused weight loss to increase rapidly in the Si-CaP and Si-CaP/FPBP group. However, after 3 days incubation, plasma PO_4^{3-} and Ca^{2+} reached heterogeneous nucleation sites and formed bone-like apatite depositions, resulting in decreased weight loss in the Si-CaP and Si-CaP/FPBP group [32]. In the period between 3 and 14 days, the FPBP of Si-CaP/FPBP group degraded and released hydroxyapatite particles that deposited on the surface of the scaffold reducing the weight loss in the Si-CaP/FPBP group compared to the Si-CaP group. The lower rate of weight loss of the Si-CaP/FPBP may be due to dense tissue structure, the presence of hydrophobic material and highly crystalline inorganic components.

Water absorption in the Si-CaP, FPBP and Si-CaP/FPBP groups increased over the first 3 days. This is probably due to a large amount of hydroxyl within the surface and internal pore wall of these porous structures which attracts water molecules through

Sun *et al. BioMed Eng OnLine* (2015) 14:47

Page 11 of 14

the process of hygroscopy [25]. Additionally, the Si-CaP group, FPBP group and Si-CaP/FPBP group had multiple micropores connected to each other, forming a capillary network structure which may absorb water by capillary action [33, 34].

The ideal autologous bone substitution materials must have good mechanical performance and changes in mechanical strength of autologous bone substitute materials should match the growth rate of bone tissue [35]. In our experiment the compressive strength and elastic modulus of the Si-CaP/FPBP group and cancellous bone group was significantly higher than that of the Si-CaP group and throughout the in vitro degradation process, there was no significant difference in compressive strength and elastic modulus between Si-CaP/FPBP group and cancellous bone group. This indicates that the addition of fine bone particles can make homogeneous composite scaffolds significantly more stress resistant. The elastic modulus of the composites was also improved by the addition of FPBP, which is advantageous in surgical applications. In addition, we observed by SEM that Si-CaP and FPBP distributed uniformly and combined to a well-knit interface. This combination and distribution at the interface provides a structural basis for good mechanical properties of Si-CaP/FPBP. Our results show that FPBP affects the degradation rate of the Si-CaP and improves its mechanical strength. Throughout the degradation process, the change in pH, weight loss, water absorption and mechanical strength indicates that Si-CaP/FPBP had better degradation and mechanical properties than Si-CaP alone.

Morphology and structure of Si-CaP/FPBP

The microstructures of porous scaffolds have been shown previously to play a vital role in new bone growth, and a pore size of at least 100 μm is a requirement for complete biological activity [36, 37]. One study reported that a scaffold exhibited osteoconductive properties when the pore size was larger than 200 μm [38]. Kang et al. [39] showed that a scaffold with 57% of porosity and pore size of 100–250 μm had good in vitro degradation performance and formed bone-like apatite. Zhuang et al. [40] found that scaffolds with 36–55% porosity and pore size of 200–400 μm had good mechanical properties and a controlled degradation rate.

The Si-CaP/FPBP scaffold constructed in our experiment had a three-dimensional porous structure with pore size about 150–300 μm ("macropores") and porosity of 75%. Macropores guide the growth of cells and blood vessel on the wall of the pore, which increases osteoconductive performance of the scaffold and bone tissue growth into the internal scaffold [41, 42]. In addition to macropores, micropores of approximately 1–10 μm were observed in the pore walls, by SEM. These micropores were channels that interconnected the larger pores of the Si-CaP/FPBP with good connectivity. Micropores have also been previously found to play important roles in osteogenesis. Yuan et al. [37] found that calcium phosphate scaffolds lacking micropores do not exhibit bone in-growth in dogs, and it is believed that micropores facilitate protein interaction, cell attachment, cellular development and orientation and directionality of cellular growth [43, 44]. Although micropores are not the osteogenic agent itself, their presence results in larger surface area which probably results in more protein absorption (for example BMP), and also ion exchange and apatite formation by dissolution and reprecipitation [37]. BMP is known to induce

Sun *et al. BioMed Eng OnLine* (2015) 14:47

Page 12 of 14

bone-formation in a dose-dependent manner with a local concentration threshold and a rough surface facilitates attachment, proliferation and differentiation of bone forming cells [37].

During the in vitro degradation process, porosity of Si-CaP/FPBP increased, the pore wall degraded, micropores formed and connectivity between pores increased. A small amount of bone-like apatite formation was observed on the surface of Si-CaP at the seventh day of degradation in DMEM culture medium. This was consistent with the reported literature in which low crystallization apatite was observed on Si-CaP on the seventh day of degradation in simulated body fluid [28]. Compared with the Si-CaP, Si-CaP/FPBP had a more rapid formation of bone-like apatite. The formation of apatite is a natural event in bone formation and important for bioactivity and differences in apatite formation rate between different Si-CaP scaffolds affects bioactivity [45].

Biological properties of Si-CaP/FPBP

In our experiment, the complete structure of osteoblasts in Si-CaP/FPBP was observed by H&E staining. After in vitro degradation for 14 days, the osteoblasts had dissolved and disappeared. In vivo studies have also shown that FPBP participates in all stages of bone defect repair,plays roles in osteogenesis [46]. Thus the addition of FPBP to Si-CaP should improve the biological activity of the scaffold and our findings support this idea.

Our data taken together and with the support of other works, show that a scaffold comprised of a porous Si-CaP structure packed with fine particles of bone provides a mileu conducive to osteogenesis, bone-bonding and bone repair, whilst maintaining mechanical strength and elastic modus. Although we only performed in vitro experiments in our studies, others have shown that such assessments correlate well with in vivo observations. Hence we expect the Si-CaP/FPBP scaffold will also perform well in vivo.

Conclusions

Si-CaP and FPBP have both been shown previously to have properties that can facilitate bone-repair. However, individually these materials are insufficient for sustaining bone remodeling. Scaffolds constructed from a combination of the two, on the other hand, may collectively possess the required characteristics for efficient bone-repair. In this study, we found that FPBP enhances the performance of a silicate-substituted calcium-phosphate scaffold. We believe that Si-CaP/FPBP scaffolds may possess the necessary characteristics required of an autologous bone graft substitute for successful bone-repair.

Authors' contributions
CS, YT, XW conceived and designed the study; CS, YT, WX, CZ and HX performed the experiments; CS, YT and WX analyzed the data; and CS, YT and XW jointly prepared the manuscript. All authors read and approved the final manuscript.

Author details
[1] Department of Orthopaedic Surgery, The Second Harbin City Hospital, Harbin 150056, China. [2] Department of Orthopaedic Surgery, The Second Affiliated Hospital of Harbin Medical University, 246 Xuefu Street, Nangang District, Harbin 150086, China.

References
1. Szpalski C, Wetterau M, Barr J, Warren SM. Bone tissue engineering: current strategies and techniques—part I: scaffolds. Tissue Eng Part B Rev. 2012;18(4):246–57.
2. Dimitriou R, Jones E, McGonagle D, Giannoudis PV. Bone regeneration: current concepts and future directions. BMC Med. 2011;9:66.
3. Venugopal J, Prabhakaran MP, Zhang Y, Low S, Choon AT, Ramakrishna S. Biomimetic hydroxyapatite-containing composite nanofibrous substrates for bone tissue engineering. Philos Trans A Math Phys Eng Sci. 1917;2010(368):2065–81.
4. Giannoudis PV, Dinopoulos H, Tsiridis E. Bone substitutes: an update. Injury. 2005;36(Suppl 3):S20–7.
5. Venkatesan J, Kim SK. Chitosan composites for bone tissue engineering—an overview. Mar Drugs. 2010;8(8):2252–66.
6. Theler JM. Bone tissue substitutes and replacements. Curr Opin Otolaryngol Head Neck Surg. 2011;19(4):317–22.
7. Bose S, Roy M, Bandyopadhyay A. Recent advances in bone tissue engineering scaffolds. Trends Biotechnol. 2012;30(10):546–54.
8. Kamitakahara M, Ohtsuki C, Miyazaki T. Review paper: behavior of ceramic biomaterials derived from tricalcium phosphate in physiological condition. J Biomater Appl. 2008;23(3):197–212.
9. Hammouche S, Hammouche D, McNicholas M. Biodegradable bone regeneration synthetic scaffolds: in tissue engineering. Curr Stem Cell Res Ther. 2012;7(2):134–42.
10. Coathup MJ, Samizadeh S, Fang YS, Buckland T, Hing KA, Blunn GW. The osteoinductivity of silicate-substituted calcium phosphate. J Bone Joint Surg Am. 2011;93(23):2219–26.
11. Jenis LG, Banco RJ. Efficacy of silicate-substituted calcium phosphate ceramic in posterolateral instrumented lumbar fusion. Spine. 2010;35(20):E1058–63.
12. Gillespie P, Wu G, Sayer M, Stott MJ. Si complexes in calcium phosphate biomaterials. J Mater Sci Mater Med. 2010;21(1):99–108.
13. Hoppe A, Guldal NS, Boccaccini AR. A review of the biological response to ionic dissolution products from bioactive glasses and glass-ceramics. Biomaterials. 2011;32(11):2757–74.
14. Maehira F, Miyagi I, Eguchi Y. Effects of calcium sources and soluble silicate on bone metabolism and the related gene expression in mice. Nutrition. 2009;25(5):581–9.
15. Honda M, Kikushima K, Kawanobe Y, Konishi T, Mizumoto M, Aizawa M. Enhanced early osteogenic differentiation by silicon-substituted hydroxyapatite ceramics fabricated via ultrasonic spray pyrolysis route. J Mater Sci Mater Med. 2012;23(12):2923–32.
16. Lehmann G, Cacciotti I, Palmero P, Montanaro L, Bianco A, Campagnolo L, et al. Differentiation of osteoblast and osteoclast precursors on pure and silicon-substituted synthesized hydroxyapatites. Biomed Mater. 2012;7(5):055001.
17. Cameron K, Travers P, Chander C, Buckland T, Campion C, Noble B. Directed osteogenic differentiation of human mesenchymal stem/precursor cells on silicate substituted calcium phosphate. J Biomed Mater Res Part A. 2013;101(1):13–22.
18. Gomes PS, Botelho C, Lopes MA, Santos JD, Fernandes MH. Evaluation of human osteoblastic cell response to plasma-sprayed silicon-substituted hydroxyapatite coatings over titanium substrates. J Biomed Mater Res B Appl Biomater. 2010;94(2):337–46.
19. Guth K, Campion C, Buckand T, Hing KA. Surface physiochemistry affects protein adsorption to stoichiometric and silicate-substituted microporous hydroxyapatites. Adv Eng Mater. 2010;12(4):B113–21.
20. Guth K, Campion C, Buckland T, Hing KA. Effect of silicate-substitution on attachment and early development of human osteoblast-like cells seeded on microporous hydroxyapatite discs. Adv Eng Mater. 2010;12(1–2):B26–36.
21. Hak DJ. The use of osteoconductive bone graft substitutes in orthopaedic trauma. J Am Acad Orthop Surg. 2007;15(9):525–36.
22. Sun YX, Sun CL, Tian Y, Xu WX, Zhou CL, Xi CY, et al. A comparison of osteocyte bioactivity in fine particulate bone powder grafts vs larger bone grafts in a rat bone repair model. Acta Histochem. 2014;116(6):1015–21.
23. Gibson IR, Best SM, Bonfield W. Chemical characterization of silicon-substituted hydroxyapatite. J Biomed Mater Res. 1999;44(4):422–8.
24. Calvo JI, Bottino A, Capannelli G, Hernandez A. Comparison of liquid–liquid displacement porosimetry and scanning electron microscopy image analysis to characterise ultrafiltration tracketched membranes. J Membr Sci. 2004;239(2):189–97.
25. Tuck L, Astala R, Reid JW, Sayer M, Stott MJ. Dissolution and re-crystallization processes in multiphase silicon stabilized tricalcium phosphate. J Mater Sci Mater Med. 2008;19(2):917–27.

Sun *et al. BioMed Eng OnLine* (2015) 14:47

Page 14 of 14

26. Bohner M. Calcium orthophosphates in medicine: from ceramics to calcium phosphate cements. Inj Int J Care Inj. 2000;31:S37–47.
27. Suchanek W, Yashima M, Kakihana M, Yoshimura M. Processing and mechanical properties of hydroxyapatite reinforced with hydroxyapatite whiskers. Biomaterials. 1996;17(17):1715–23.
28. Patel N, Brooks RA, Clarke MT, Lee PM, Rushton N, Gibson IR, et al. In vivo assessment of hydroxyapatite and silicate-substituted hydroxyapatite granules using an ovine defect model. J Mater Sci Mater Med. 2005;16(5):429–40.
29. Samachson J. Basic requirements for calcification. Nature. 1969;221(5187):1247–8.
30. Kokubo T, Takadama H. How useful is SBF in predicting in vivo bone bioactivity? Biomaterials. 2006;27(15):2907–15.
31. Loty C, Sautier JM, Boulekbache H, Kokubo T, Kim HM, Forest N. In vitro bone formation on a bone-like apatite layer prepared by a biomimetic process on a bioactive glass-ceramic. J Biomed Mater Res. 2000;49(4):423–34.
32. Pilliar RM, Filiaggi MJ, Wells JD, Grynpas MD, Kandel RA. Porous calcium polyphosphate scaffolds for bone substitute applications—in vitro characterization. Biomaterials. 2001;22(9):963–72.
33. Deb S, Braden M, Bonfield W. Water absorption characteristics of modified hydroxyapatite bone cements. Biomaterials. 1995;16(14):1095–100.
34. Lockington DA, Parlange JY. Anomalous water absorption in porous materials. J Phys D Appl Phys. 2003;36:760–7.
35. Liu X, Huang W, Fu H, Yao A, Wang D, Pan H, et al. Bioactive borosilicate glass scaffolds: in vitro degradation and bioactivity behaviors. J Mater Sci Mater Med. 2009;20(6):1237–43.
36. Shore EC, Holmes E. Porous hydroxyapatite. Singapore: World Scientific; 1993.
37. Yuan H, Kurashina K, de Bruijn JD, Li Y, de Groot K, Zhang X. A preliminary study on osteoinduction of two kinds of calcium phosphate ceramics. Biomaterials. 1999;20(19):1799–806.
38. Zhang F, Chang J, Lin K, Lu J. Preparation, mechanical properties and in vitro degradability of wollastonite/tricalcium phosphate macroporous scaffolds from nanocomposite powders. J Mater Sci Mater Med. 2008;19(1):167–73.
39. Kang Y, Yao Y, Yin G, Huang Z, Liao X, Xu X, et al. A study on the in vitro degradation properties of poly(L-lactic acid)/beta-tricalcuim phosphate (PLLA/beta-TCP) scaffold under dynamic loading. Med Eng Phys. 2009;31(5):589–94.
40. Zhuang HY, Han Y, Feng AL. Preparation, mechanical properties and in vitro biodegradation of porous magnesium scaffolds. Mat Sci Eng C Bio S. 2008;28(8):1462–6.
41. Shen J, Li Y, Zuo Y, Zou Q, Cheng L, Zhang L, et al. Characterization and cytocompatibility of biphasic calcium phosphate/polyamide 6 scaffolds for bone regeneration. J Biomed Mater Res B Appl Biomater. 2010;95(2):330–8.
42. Lu JX, Flautre B, Anselme K, Hardouin P, Gallur A, Descamps M, et al. Role of interconnections in porous bioceramics on bone recolonization in vitro and in vivo. J Mater Sci Mater Med. 1999;10(2):111–20.
43. Sanchez-Salcedo S, Nieto A, Vallet-Regi M. Hydroxyapatite/β-tricalcium phosphate/agarose macroporous scaffolds for bone tissue engineering. Chem Eng J. 2008;137:62–71.
44. Sánchez-Salcedo S, Arcos D, Vallet-Regí M. Upgrading calcium phosphate scaffolds for tissue engineering applications. Key Eng Mater. 2008;377:19–42.
45. Oyane A, Kawashita M, Nakanishi K, Kokubo T, Minoda M, Miyamoto T, et al. Bonelike apatite formation on ethylene–vinyl alcohol copolymer modified with silane coupling agent and calcium silicate solutions. Biomaterials. 2003;24(10):1729–35.
46. Wang XT, Zhou CL, Yan JL, Yan X, Xie HX, Sun CL. The fate of donor osteocytes in fine particulate bone powders during repair of bone defects in experimental rats. Acta Histochem. 2012;114(3):192–8.